

Crescent-shaped spot modeling of runaway electron synchrotron radiation

I.M. Pankratov^{1,2}, V.Y. Bochko¹

¹*V.N. Karazin Kharkiv National University, 61022 Kharkiv, Ukraine*

²*Institute of Plasma Physics, NSC “Kharkiv Institute of Physics and Technology”, Akademichna str., 1, 61108 Kharkiv, Ukraine*

Introduction: The energy of disruption generated runaway electrons (REs) can reach as high as tens of MeV and they can cause serious damage to plasma-facing surfaces in large tokamaks and ITER (see, e. g., [1]). At the same time, the quiescent RE generation in low density Ohmic discharges is used for a more detailed and accurate measurement of RE parameters (see, e.g., [2]). The investigation of RE synchrotron radiation spot allows studying the parameters: RE beam size and position, number, and maximum energy of REs. The parameter $\theta_p = v_\perp / |v_\parallel|$ (pitch angle) strongly influences the RE synchrotron radiation behavior (v_\parallel is the longitudinal velocity, v_\perp is the transverse velocity with respect to the magnetic field \vec{B}). Because in tokamak experiments the strong inequality $\theta_p \gg \gamma^{-1}$ takes place, the small uncertainty introduced by the angular broadening of radiation, $\sim \gamma^{-1}$, is possible to neglect (cone model), γ is the relativistic factor. The case of the small parameter $\theta_p \ll 1$ (linear cone model) was considered in [3] and is used for experimental data analysis till now.

In the recent papers (see, e.g., [2,4]), a large pitch angle ($\theta_p \sim 1$) was declared for the observed synchrotron emission (SE) crescent-shaped spots. And in [5] it was revealed that the dominating particle should have a $\theta_p \sim 0.35$ rad, $E=25$ MeV (DIII-D, # 165826).

Nonlinear cone model equations: For the RE finite pitch angle values the analytical expressions for analysis of the SE in tokamaks have been obtained in [6] (nonlinear cone model, $\theta_p \sim 1$), $\zeta = \pi/2 + \Delta$, see Fig. 1. They have the next form ($\dot{\alpha} \approx \omega_B$, $\omega_B(r, \theta) = eB(r, \theta)/\gamma m_e c$ ($e > 0$), D is the distance from the detector to YZ plane):

$$\begin{aligned} & \pm \left[r \sin \theta \mp \frac{v_\perp}{\omega_B} \cos(\theta \pm \alpha) - Z_{\text{det}} \right] \left[\cos \Delta \mp \frac{v_\perp}{v_\parallel} \sin \Delta \cos(\theta \pm \alpha) \right] = \\ & = \left[D + (R_0 - r \cos \theta) \sin \Delta \right] \left[\frac{r}{qR_0} \cos \theta + \frac{v_\perp}{v_\parallel} \sin(\theta \pm \alpha) \mp \frac{1}{v_\parallel} \frac{v_\parallel^2 + 0.5v_\perp^2}{\omega_B R_0} \pm \frac{v_\perp}{v_\parallel} \frac{v_\perp}{\omega_B r} \cos(\theta \pm \alpha) \cos \alpha \right], \end{aligned} \quad (1)$$

$$\sin \Delta \left[1 \pm \frac{Y_{\text{det}}}{D} \frac{v_\perp}{v_\parallel} \cos(\theta \pm \alpha) \right] = \frac{Y_{\text{det}} \cos \Delta - (R_0 - r \cos \theta)}{D} \mp \frac{v_\perp}{v_\parallel} \cos \Delta \cos(\theta \pm \alpha), \quad (2)$$

The tokamak confinement magnetic field is presented in the form:

$$\vec{B}(r, \vartheta) = B_{0\zeta} R_0 / R \left(\pm \vec{e}_\zeta + r / q(r) R_0 \vec{e}_\theta \right). \quad (3)$$

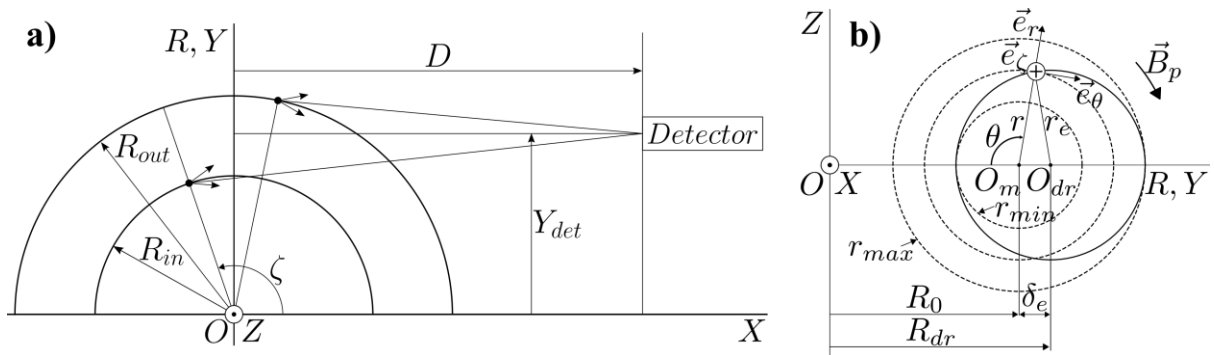


Figure 1. a) Relative positions of the runaway electrons beam and the detector are shown. For simplicity, the case of the plane $z=0$ ($Z_{\text{det}}=0$) is presented, R_{in} and R_{out} are the inner and outer major radii of the beam in this plane, the cones of radiation emitted by electrons are represented schematically; b) the cross-sections (through the plane $\zeta=\pi/2$) of the magnetic surfaces (dashed circles) with a center at the point O_m and the drift surface with shift δ_e (solid circle) at a center O_{dr} are plotted, r_{min} and r_{max} are minimal and maximal minor radii of magnetic surfaces corresponding to this drift surface with radius r_e . The X-axis is directed toward the detector. The direction of the poloidal magnetic field \vec{B}_p is shown.

The upper signs in the Eqs. (1-3) correspond to the case when the magnetic field \vec{B} is directed away from the detector, and for the lower signs field is directed toward the detector. For the RE moving toward the detector the longitudinal velocity v_{\parallel} is negative for the upper sign ($v_{\parallel} < 0$) and positive for the lower sign ($v_{\parallel} > 0$). The RE motion along the tokamak helical magnetic field with velocity v_{\parallel} , cyclotron gyration motion around the guiding centre with the velocity v_{\perp} , safety factor $q(r)$, the horizontal displacement of the RE drift surfaces with respect to the magnetic surfaces, and the position of the detector are taken into account.

Note that besides the parameter $v_{\perp}/|v_{\parallel}|$, the ratio Y_{det}/D is also the key parameter for the analysis of the synchrotron radiation spot shape and that for each poloidal angle θ the SE of REs is detected by the camera for certain values of α (cyclotron rotation angle) only.

Modeling of DIII-D experiment: The results of [6] are used for qualitative modeling of the DIII-D experiment [2], shot #152893, $\lambda = 901\text{nm}$ where the SE crescent-shaped spot was observed (Fig. 5 in [2]) on the high-field side (HFS). Our calculations confirmed the result of [2]: when REs reached $E = 30$ MeV REs were no longer confined in the tokamak (see Fig. 2). The REs must have energy $E \gtrsim 25$ MeV to emit visible SE and be detected in the DIII-D experiment. That is why in Fig. 3 we present the SE spot modeling for RE energies 25 and 30 MeV. The SE is found in [2] to be absent from approximately inside the $q = 1$ surface and outside the $q = 3$ surface. In Fig. 2 the drift orbits are the solution of relativistic drift motion equations. In modeling, the starting points of REs drift orbits are on the HFS between $q = 1$ and $q = 1.5$ magnetic surfaces.

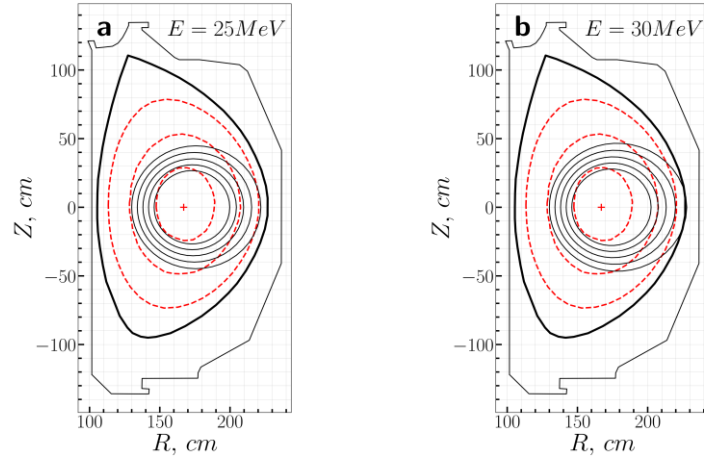
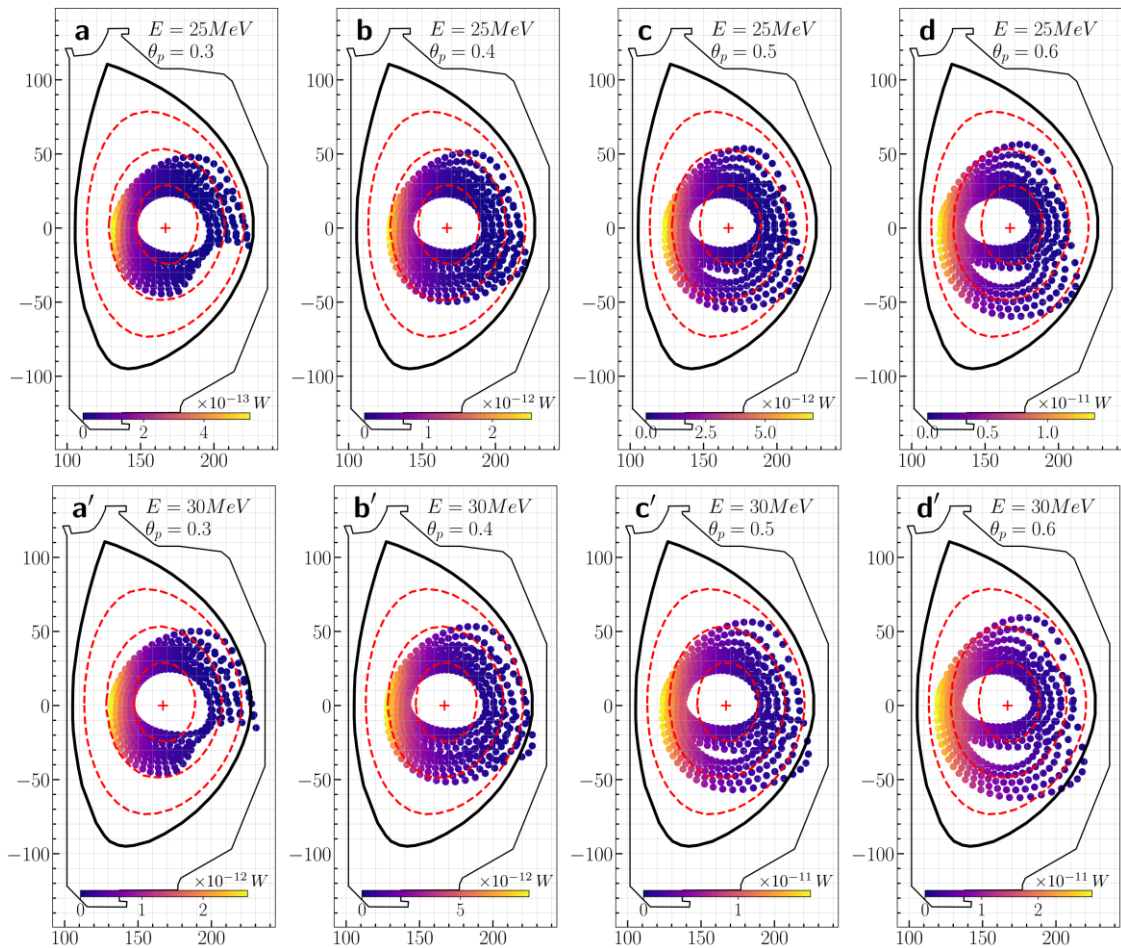


Figure 2. Modeling of runaway electron drift orbits for energies a) 25 MeV and b) 30 MeV.

Figure 3. Modeling of synchrotron spots. For $\theta_p = 0.6$ the bright edge of SE spot is shifted to $q = 3$ like in Fig. 5(f) [2].

The magnetic surfaces $q = 1, 1.5$ and 3 are shown in Figs. 2,3 by red dashed lines. The values $0.3, 0.4, 0.5$ and 0.6 of parameter θ_p were assigned at the $q = 1.5$ surface only and were varied along RE drift orbits according to the conservation of magnetic moment. The color of each

point in Fig. 3 corresponds to the value of $\int_{\lambda_{\min}}^{\lambda_{\max}} d\lambda P(\lambda)$, where $(\lambda_{\min}, \lambda_{\max})$ – detector's

wavelength range and $P(\lambda) = i \frac{2\pi ce^2}{\lambda^3 \gamma^2} \left\{ \int_C^{\lambda} \frac{du}{u} (1 - 2u^2) I_0(au^3) \exp \left[-\frac{3}{2} \xi \left(u - \frac{u^3}{3} \right) \right] - \frac{4\eta}{1 + \eta^2} \int_C^{\lambda} du \cdot u I_1(au^3) \exp \left[-\frac{3}{2} \xi \left(u - \frac{u^3}{3} \right) \right] \right\}$ is the full equation of spectral density [7],

where $a = \frac{\xi\eta}{1 + \eta^2}$, $\xi = \frac{4\pi R}{3\lambda\gamma^3\sqrt{1 + \eta^2}}$, $\eta = \frac{v_{\perp}}{v_{dr}}$ and $v_{dr} = \frac{v_{\parallel}^2 + 0.5v_{\perp}^2}{\omega_B R_0}$.

Conclusions: Presented results show that a crescent shape appears for a large pitch angle ($\theta_p \sim 1$) and the relative absence of SE on the magnetic field LFS is an artifact of the conservation of magnetic momentum. Our calculations confirm the statements of Refs. 2,4,5.

A good agreement between the presented qualitative modeling and the DIII-D experiment [2] is obtained. In our opinion, the synchrotron radiation crescent-shaped spot shown in Fig. 5(f) corresponds to the value of parameter $v_{\perp}/|v_{\parallel}| \approx 0.6$.

The values $v_{\perp}/|v_{\parallel}|$ and Y_{det}/D are the key parameters for the analysis of the synchrotron radiation spot shape.

Acknowledgments. Authors thanks Z. Popovic for useful and fruitful discussions.

References

- [1] B.N. Breizman, P. Aleynikov, E.M. Hollmann et al, Physics of runaway electrons in tokamaks, Nuclear Fusion, **59**, 083001 (2019)
- [2] C. Paz-Soldan, N.W. Eidietis, R. Granetz et al, Growth and decay of runaway electrons above the critical electric field under quiescent conditions, Phys. Plasmas **21**, 022514 (2014)
- [3] I.M. Pankratov, Analysis of the synchrotron radiation emitted by runaway electrons, Plasma Physics Reports, **22**, 535 (1996)
- [4] J.H. Yu, E.M. Hollmann, N. Commaux et al, Visible imaging and spectroscopy of disruption runaway electrons in DIII-D, Phys. Plasmas **20**, 042113 (2013)
- [5] M. Hoppe, O. Embréus, C. Paz-Soldan et al, Interpretation of runaway electron synchrotron and bremsstrahlung images, Nuclear Fusion, **58**, 082001 (2018)
- [6] I.M. Pankratov, V.Y. Bochko. Nonlinear cone model for investigation of runaway electron synchrotron radiation spot shape, East European J. of Phys., No.3, p. 20 (2021), doi.org/10.26565/2312-4334-2021-3-02
- [7] I.M. Pankratov, Analysis of the synchrotron radiation spectra of runaway electrons, Plasma Physics Reports **25**, 145 (1999)